Molecular Cell *21*, 481–493, February 17, 2006 ©2006 Elsevier Inc. DOI 10.1016/j.molcel.2006.01.012

PKC Regulates a Farnesyl-Electrostatic Switch on K-Ras that Promotes its Association with Bcl-X_L on Mitochondria and Induces Apoptosis

Trever G. Bivona,[2,7] Steven E. Quatela,[3,7] Brian O. Bodemann,[5] Ian M. Ahearn,[2] Michael J. Soskis,[2] Adam Mor,[1] John Miura,[3] Heidi H. Wiener,[2] Latasha Wright,[2] Shahryar G. Saba,[2] Duke Yim,[2] Adam Fein,[2] Ignacio Pérez de Castro,[4,8] Chi Li,[6] Craig B. Thompson,[6] Adrienne D. Cox,[5] and Mark R. Philips[1,2,3,*]

[1] Department of Medicine
[2] Department of Cell Biology
[3] Department of Pharmacology
[4] Department of Pathology
New York University School of Medicine
550 First Avenue
New York, New York 10016
[5] Departments of Radiation Oncology and Pharmacology
University of North Carolina at Chapel Hill School of Medicine
101 Manning Drive
Chapel Hill, North Carolina 27599
[6] Department of Cancer Biology
University of Pennsylvania School of Medicine
421 Curie Boulevard
Philadelphia, Pennsylvania 19104

Summary

K-Ras associates with the plasma membrane (PM) through farnesylation that functions in conjunction with an adjacent polybasic sequence. We show that phosphorylation by protein kinase C (PKC) of S181 within the polybasic region promotes rapid dissociation of K-Ras from the PM and association with intracellular membranes, including the outer membrane of mitochondria where phospho-K-Ras interacts with Bcl-X_L. PKC agonists promote apoptosis of cells transformed with oncogenic K-Ras in a S181-dependent manner. K-Ras with a phosphomimetic residue at position 181 induces apoptosis via a pathway that requires Bcl-X_L. The PKC agonist bryostatin-1 inhibited the growth in vitro and in vivo of cells transformed with oncogenic K-Ras in a S181-dependent fashion. These data demonstrate that the location and function of K-Ras are regulated directly by PKC and suggest an approach to therapy of K-Ras-dependent tumors with agents that stimulate phosphorylation of S181.

Introduction

Although mammalian genomes contain three *ras* genes, mutations in *K-ras* are most frequently associated with human cancer (Bos, 1989). The differential biology of Ras isoforms is generated in large part by distinct membrane-targeting sequences. Membrane association of all Ras isoforms requires farnesylation, proteolysis, and carboxyl methylation of a C-terminal CAAX motif. Plasma membrane (PM) targeting of the principal splice variant of K-Ras also requires a unique polybasic region adjacent to the CAAX motif (Choy et al., 1999; Hancock et al., 1990; Jackson et al., 1994). K-Ras thus falls into a broad class of proteins that are anchored to the cytoplasmic face of the PM by virtue of posttranslational modification with lipids that act in conjunction with polybasic stretches of polypeptide. Whereas the lipid moieties are thought to insert into the phospholipid bilayer, the polybasic regions are believed to associate with the anionic head groups of inner leaflet phospholipids (Leventis and Silvius, 1998). Included in this class of proteins is the myristoylated alanine-rich C kinase substrate (MARCKS) that associates with the PM via an N-terminal myristoyl modification and a polybasic region. Serine residues within the polybasic region are sites for PKC-mediated phosphorylation (Figure 1A) that neutralize the charge and thereby cause the MARCKS protein to dissociate from the PM. The mechanism by which MARCKS is discharged from the PM through phosphorylation has been referred to as a myristoyl-electrostatic switch (McLaughlin and Aderem, 1995).

Like MARCKS, the polybasic region of K-Ras harbors three potential phosphorylation sites, and this segment has previously been shown to be phosphorylated by PKC (Ballester et al., 1987). We therefore tested the hypothesis that phosphorylation of the C-terminal segment of K-Ras might regulate its association with the PM and thereby constitute a farnesyl-electrostatic switch. We observed that PKC agonists induced a rapid translocation of K-Ras from the PM to intracellular membranes that included the endoplasmic reticulum (ER) and Golgi apparatus. Surprisingly, the membranes upon which phosphorylated K-Ras accumulated also included the outer mitochondrial membrane where K-Ras associated with Bcl-X_L. Furthermore, phosphorylation and internalization of K-Ras stimulated apoptosis in a Bcl-X_L-dependent fashion. Finally, we show that a PKC agonist with established anticancer activity limits the growth of tumors driven by activated K-Ras with a wild-type membrane-targeting region but not oncogenic K-Ras with an alanine substitution at the principal PKC site. These observations show that the subcellular localization and function of K-Ras are modulated by PKC.

Results

PKC Agonists Modulate the Association of K-Ras with the PM

To determine if PKC activation could affect the localization of K-Ras in a fashion analogous to MARCKS, we expressed K-Ras tagged with green fluorescent protein (GFP) in a variety of cell types and observed its subcellular localization in living cells before and after stimulation of PKC. We used bryostatin-1, a potent PKC agonist that, like phorbol esters, binds to the C1 regulatory domains of PKCs and promotes their association with membranes (Kortmansky and Schwartz, 2003). Before

*Correspondence: philim01@med.nyu.edu
[7] These authors contributed equally to this work.
[8] Present address: Molecular Oncology Program, Spanish National Cancer Center, Melchor Fernandez Almagro, 3, 28029 Madrid, Spain.

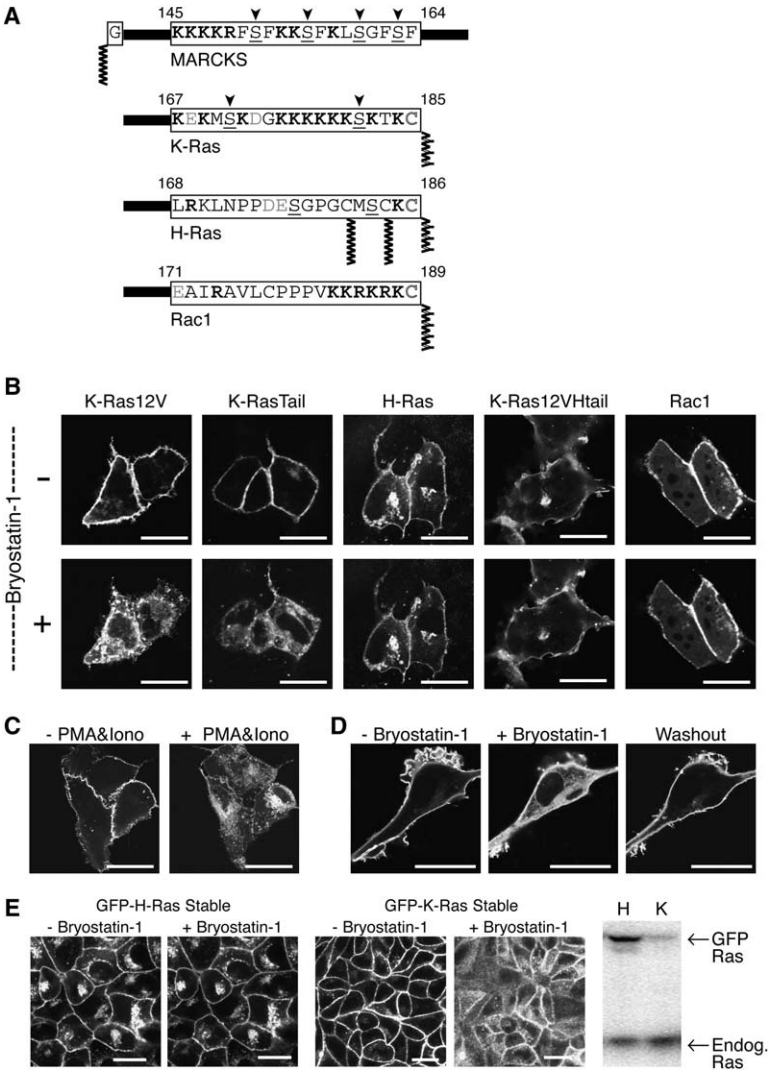

Figure 1. PKC Agonists Stimulate Translocation of K-Ras from the PM to Internal Membranes

(A) Comparison of the membrane-targeting sequences present in the MARCKS protein with K-Ras, H-Ras, and Rac1. Arrowheads indicate putative PKC sites.

(B) Effect of bryostatin-1 (0 and 3 min) on localization of the indicated constucts in MDCK cells.

(C) PMA and ionomycin promote internalization of GFP-K-Ras12V.

(D) Effect of bryostatin-1 is reversible (10 min washout).

(E) Bryostatin-1 (1 μM, 5 min) induced translocation of GFP-K-Ras but not GFP-H-Ras expressed at endogenous levels (IB, right panel) in MDCK cells. Bars, 10 μm.

stimulation, GFP-K-Ras was observed almost exclusively at the PM. Bryostatin-1 induced a rapid (<1 min onset, 3 min maximal) translocation of the GTPase from the PM to intracellular membranes (Figure 1B). Phorbol myristate acetate (PMA) had a similar but much weaker effect, consistent with its lower potency relative to bryostatin-1 (Szallasi et al., 1994). However, when PMA was combined with the calcium ionophore ionomycin, known to synergize with PMA in stimulating PKCs, the effects on GFP-K-Ras localization were identical to those of bryostatin-1 (Figure 1C). GFP extended with the 20 amino acid C terminus of K-Ras behaved in a manner identical to that of full-length GFP-K-Ras, demonstrating that all of the information required for both PM targeting and translocation in response to PKC activation was contained in this region. Neither H-Ras, an isoform lacking a polybasic region, nor Rac1, a Ras-related GTPase with a polybasic region devoid of phosphorylation sites (Figure 1A), was redistributed in response to PKC agonists (Figure 1B). The localization of K-Ras extended beyond its CAAX sequence with the hypervariable region of H-Ras was also unaffected by PKC agonists (Figure 1B), demonstrating that the H-Ras membrane anchor is dominant when placed in tandem with the K-Ras polybasic region. The effect of bryostatin-1 on K-Ras localization was reversible (Figure 1D), consistent with a phosphorylation/dephosphorylation cycle, a conclusion also supported by the observation that the phosphatase inhibitor, okadaic acid, induced partial internalization of GFP-K-Ras (data not shown). To rule out the possibility that the translocation we observed was a consequence of the overexpression of the GFP-tagged proteins, we produced MDCK cell lines that stably express GFP-H-Ras or GFP-K-Ras at levels at or below those of the endogenous proteins (Figure 1E, right panel). In these cells, whereas bryostatin-1 induced internalization of a significant portion of GFP-K-Ras, the subcellular distribution of H-Ras was unaffected (Figure 1E). Thus, PKC agonists dynamically regulate the association of K-Ras with the PM via its C-terminal segment.

PKC-Mediated Phosphorylation of K-Ras on S181 Promotes K-Ras Internalization

The synergistic effect of ionomycin on PMA-induced K-Ras translocation raised the possibility that calcium might play a role beyond the activation of PKCs, since calmodulin has been shown to associate with (Villalonga

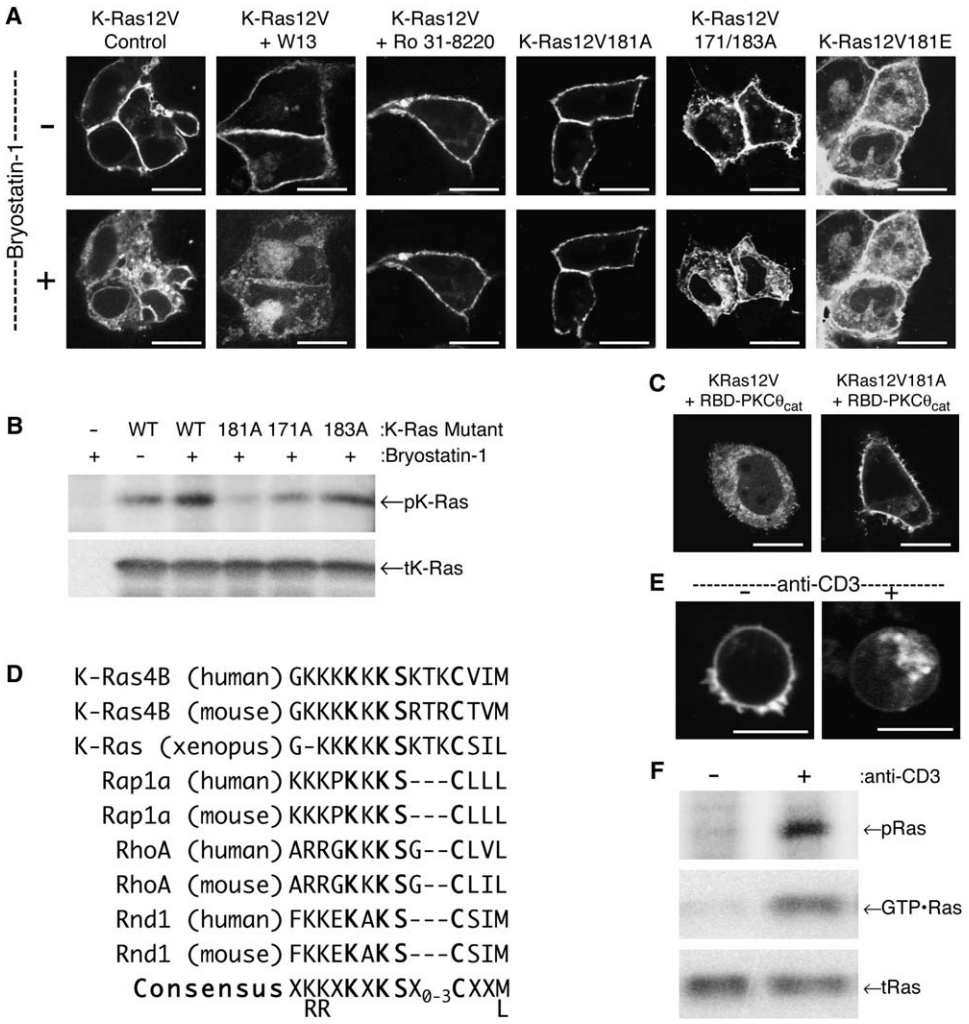

Figure 2. PKC Phosphorylates K-Ras on S181 to Promote Internalization

(A) Effect of bryostatin-1 (0 and 3 min) on localization of the indicated constucts in MDCK cells with or without pretreatment with an inhibitor of calmodulin (W-13) or PKC (Ro-31-8220).

(B) IP of the K-Ras construct indicated from lysates of COS-1 cells metabolically labeled with [^{32}P]orthophosphate and treated ± bryostatin-1.

(C) Expression of RBD-PKCθ_{cat} promotes constitutive internalization of GFP-K-Ras12V but not GFP-K-Ras12VS181A.

(D) Sequence alignment of Ras-related GTPases reveals potential PKC phosphorylation sites.

(E) Crosslinking of the antigen receptor on Jurkat T cells stimulated internalization of GFP-K-Ras (29% ± 1% of cells).

(F) TCR crosslinking of Jurkat cells stimulated [^{32}P] incorporation into endogenous Ras (top panel). The same conditions also stimulated GTP loading of Ras (middle panel). Bars, 10 μm.

et al., 2001) and extract (Fivaz and Meyer, 2005; Sidhu et al., 2003) K-Ras from membrane fractions in vitro, a process antagonized by calmodulin inhibitors. Although bryostatin-1 is not known to mobilize intracellular calcium, suggesting that PKC activation is sufficient for K-Ras translocation, we nevertheless tested the role of calmodulin. Pharmacologic inhibition of calmodulin affected neither PMA+Iono nor bryostatin-1-stimulated (Figure 2A) translocation of K-Ras, suggesting that calmodulin does not play a role. In contrast, the PKC inhibitor Ro 31-8220 completely blocked K-Ras translocation (Figure 2A).

Although the effects of PKC activation on K-Ras localization could be indirect, the previous demonstration of a PKC substrate in the C terminus of K-Ras (Ballester et al., 1987) suggested that the effect is more likely direct. The C-terminal region of K-Ras harbors three potential phosphate acceptors, S171, S181, and T183 (Figure 1A), although only the serines conform to consensus phosphorylation sites and previous phosphoamino acid analysis of K-Ras from cells exposed to PKC agonists revealed only phosphoserine (Ballester et al., 1987). Within the C-terminal membrane-anchoring region of K-Ras, S181 conforms most closely to a consensus PKC site. Whereas substitution of alanine for serine at position 181 completely blocked bryostatin-1-induced translocation of GFP-K-Ras, double substitution of S171 and T183 for alanines did not inhibit K-Ras internalization (Figure 2A). Substitution of glutamic acid for S181 to create a phosphomimetic residue resulted in a form of K-Ras that was constitutively associated with internal membranes (Figure 2A). These data suggest that K-Ras is a direct substrate for PKC and that phosphorylation of S181 mediates translocation.

To confirm phosphorylation of S181 of K-Ras, we performed metabolic labeling with [^{32}P]orthophosphate. Bryostatin-1 induced phosphorylation of K-Ras that was markedly diminished with an S181A substitution, confirming S181 as the major phosphate acceptor (Figure 2B). However, the low level of ^{32}P incorporation into the 181A mutant suggests that, although S181 is the primary site, other minor sites of phosphorylation are likely. The diminished signal in the S171A mutant suggested that this residue also serves as a phosphate acceptor. In contrast, a T183A substitution did not diminish ^{32}P incorporation, confirming that phosphorylation of this residue is not involved in regulating K-Ras localization. Phosphomimetic (glutamic acid) substitution of S171 resulted in some constitutive internalization, although substitution of S181 was more efficient in this regard, and a double mutant, GFP-K-Ras12V171E181E, was indistinguishable from GFP-K-Ras12V181E (data not shown). Together, our data suggest that, whereas reversible phosphorylation of S181 is both necessary and sufficient to cause K-Ras translocation, phosphorylation of S171 may also contribute.

The sufficiency of a single phosphorylation event for discharge of K-Ras from the PM suggested that the basal affinity for the PM conferred by the polybasic region is relatively low. To test this idea, we metabolically labeled cells with [^{35}S]methionine and tracked by subcellular fractionation and immunoprecipitation the localization of GFP-K-Ras stably expressed at a level equivalent to the endogenous protein (Figure 1E). After steady-state labeling (17 hr), 23.8% ± 6.8% (mean ± SEM, n = 3) of GFP-K-Ras was recovered in the high-speed supernatant. Moreover, when the high-speed pellet was rehomogenized with unlabeled, isotonic cytosol and then recovered by centrifugation, 39% ± 5% (mean ± SEM, n = 4) was recovered in the second high-speed supernatant. These data suggest that the binding affinity of K-Ras for membranes is relatively low such that a partial neutralization of the polybasic region could be sufficient to significantly affect the overall membrane affinity.

Next, we reasoned that if bryostatin-1 induces internalization of K-Ras via recruitment and activation of PKC at the PM where K-Ras resides, then targeting PKC to K-Ras in a bryostatin-independent fashion should promote constitutive internalization. To test this idea, we expressed the catalytic domain of PKCθ fused with the Ras binding domain (RBD) of Raf-1 and found that, in cells expressing this construct, GFP-K-RasV12 with a wild-type C terminus was partially internalized, but GFP-K-Ras12V181A was not (Figure 2C). This result confirms that S181 is a PKC site and that its phosphorylation is necessary and sufficient for PKC-induced translocation of K-Ras to internal membranes.

Our data suggest that PKC regulates the subcellular localization of K-Ras via a farnesyl-electrostatic switch analogous to the myristoyl-electrostatic switch that regulates the localization of MARCKS. Evolutionarily conserved, consensus phosphorylation sites analogous to S181 of K-Ras are also found in Ras-related proteins of both the Ras and Rho families, suggesting that a prenyl-electrostatic switch may be a general mechanism for a subclass of GTPases (Figure 2D). Indeed, phosphorylation of these sites in Rap1a (Lerosey et al., 1991; Quilliam et al., 1991) and RhoA (Lang et al., 1996) has been reported. Moreover, we have observed PKC-dependent Rnd3 translocation from the PM to internal membranes that can be mimicked by substituting a negatively charged residue for the Rnd3 serine at the position analogous to S181 of K-Ras (A.D.C., unpublished data).

T Cell Signaling Induces K-Ras Internalization and Ras Phosphorylation

To verify that the effect observed by direct activation of PKC with diacylglycerol analogs reflected physiologic signaling, we studied lymphocytes that are well known to activate both Ras (Downward et al., 1990) and PKC (Valge et al., 1988) following engagement of the T cell receptor (TCR). GFP-K-Ras expressed on the PM of Jurkat T cells was observed in 29% ± 1% (mean ± SEM, n = 4) of cells to rapidly (<5 min) translocate to internal membranes in response to crosslinking of the TCR with anti-CD3 antibodies (Figure 2E). Both phosphorylation and GTP loading of endogenous Ras were observed in Jurkat T cells following stimulation of the TCR (Figure 2F), demonstrating Ras phosphorylation in response to physiological signaling.

PKC Induces Translocation of K-Ras from the PM to ER, Golgi, and Mitochondria

Because farnesylated K-Ras that lacks a polybasic sequence in the C-terminal hypervariable region localizes on the ER and Golgi apparatus (Choy et al., 1999), we predicted that these would be the intracellular compartments upon which phosphorylated K-Ras accumulates. Indeed, the clear decoration of the nuclear envelope with GFP-K-Ras in cells treated with bryostatin-1 identified the ER as one target compartment (Figures 1B and 2A). This was confirmed by colocalization of YFP-K-Ras with a CFP-tagged ER marker in bryostatin-1-treated cells (Figure 3A). Similarly, association with the Golgi apparatus was demonstrated with a CFP-tagged Golgi marker (Figure 3A). However, the ER and Golgi localization did not account for all of the internalized K-Ras. Also apparent were widely scattered structures that had a vesicular appearance. Unexpectedly, these structures proved to be mitochondria, as demonstrated by colocalization with MitoTracker Red (Figure 3A). The fluorescence pattern around the rim of mitochondria marked by MitoTracker Red suggested localization on the outer mitochondrial membrane (Figure 3A, insert). To rule out the possibility that the mitochondrial localization was a function of GFP-K-Ras overexpression, we examined MDCK cell lines that stably express GFP-K-Ras or GFP-H-Ras at or below endogenous levels. As in the transiently transfected cells, bryostatin-1 stimulated rapid association of GFP-K-Ras but not GFP-H-Ras with mitochondria (Figure 3B).

To determine if endogenous Ras localizes on mitochondria in a PKC-dependent fashion, we performed immunogold EM studies on Jurkat T cells (Figure 3C). In untreated cells, we observed 6.4 ± 0.5 (mean ± SEM, n = 8) 10 nm gold particles/μm^2 of cytoplasm (excluding PM), of which less than one in three were associated with mitochondria. In bryostatin-1-treated cells, we observed 31.0 ± 1.1 gold particles/μm^2, of which 49% were associated with mitochondria ($p < 0.001$)

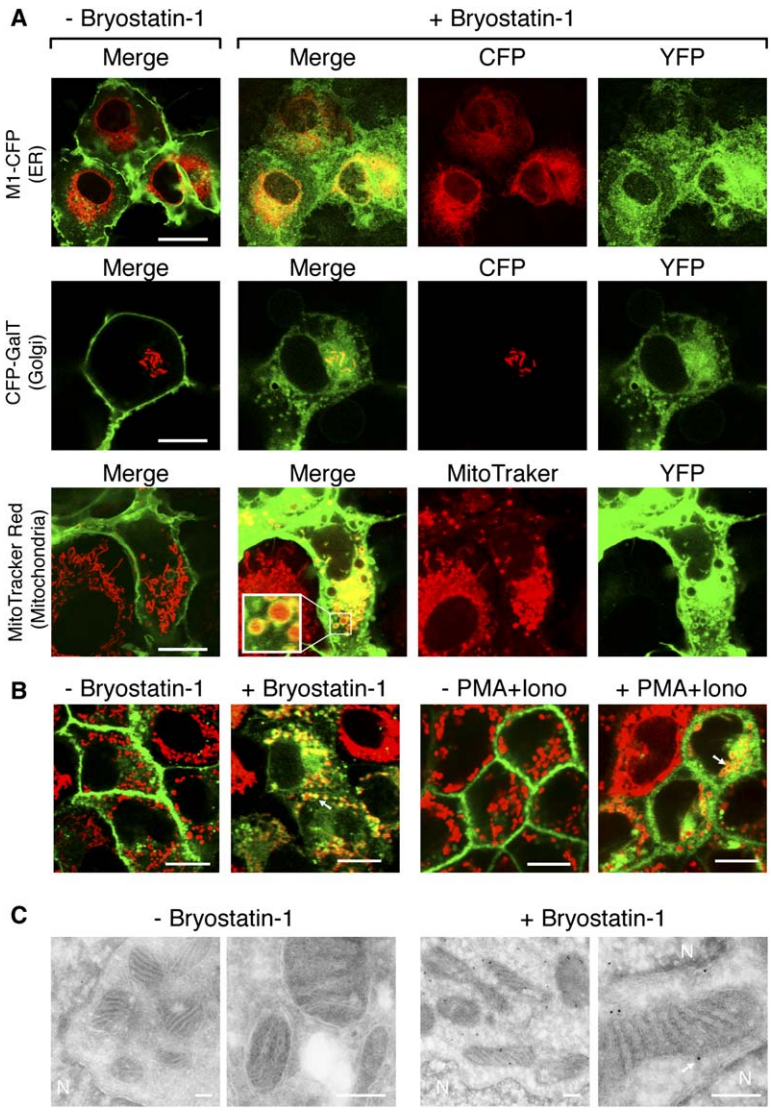

Figure 3. Phosphorylation of K-Ras Promotes Translocation from PM to ER, Golgi, and Mitochondria

(A) COS-1 cells expressing YFP-K-Ras12V and the indicated CFP-tagged compartment marker or treated with MitoTracker Red were treated with bryostatin-1 (0 and 6 min). Inset shows localization on the outer mitochondrial membrane. (B) Both bryostatin-1 and PMA + ionomycin stimulated translocation to mitochondria (arrows) in MDCK cells expressing GFP-K-Ras at levels below endogenous. (A and B) Bars, 10 μm. (C) Anti-Ras immunogold electron micrographs of Jurkat T cells before and after treatment with bryostatin-1. Arrow, 10 nm gold particle; N, nucleus; bars, 200 nm.

and the rest with ER, Golgi, and nuclear envelope. Of the mitochondria-associated gold particles in bryostatin-1-treated cells, 81% were located within 30 nm of the outer mitochondrial membrane, confirming the fluorescence results and demonstrating PKC-dependent association of endogenous Ras with mitochondria. Although the only antibody that proved useful in the immunogold EM study was a pan-Ras antibody, the fluorescent studies strongly suggest that the endogenous Ras observed on mitochondria was K-Ras.

Phosphorylated K-Ras Promotes Apoptosis

We have shown that Ras proteins can signal from endomembranes (Bivona et al., 2003; Chiu et al., 2002). Accordingly, we sought to determine the signaling characteristics of K-Ras internalized via its farnesyl-electrostatic switch. The protean effects of PKC agonists on signaling pathways make interpretation of experiments utilizing these agents difficult. We therefore sought to specifically determine the effects of phosphorylation on S181 on K-Ras signaling by expressing phosphomimetic K-Ras12V181E and testing its function. However, this approach proved impracticable because of the surprising observation that expression of K-Ras12V181E was highly toxic to cells. Ras proteins have been found to regulate both anti- and proapoptotic signaling (Cox and Der, 2003). We therefore tested the possibility that the observed toxicity was a result of apoptosis. Overexpression of Bcl-2 (Figure 4A) or a caspase-3/7 inhibitor (data not shown) blocked the toxicity of K-Ras12V181E, implicating apoptosis.

To confirm that K-Ras phosphorylated at S181 could induce apoptosis, we utilized a YFP-tagged caspase-3 sensor that localizes in the cytosol of healthy cells but enters the nucleus of cells undergoing apoptosis (Vos et al., 2003a). Exposure of COS-1 cells to UV light induced translocation of the caspase sensor into the nucleus (Figure 4B). UV exposure of cells expressing GFP-K-Ras induced apoptosis but did not induce internalization of the GTPase (data not shown), demonstrating that internalization of K-Ras is not a general consequence of apoptosis. Expression of activated H-Ras61L resulted in a relatively low apoptotic index similar to that of vector transfected cells (Figures 4B and 4C). In contrast,

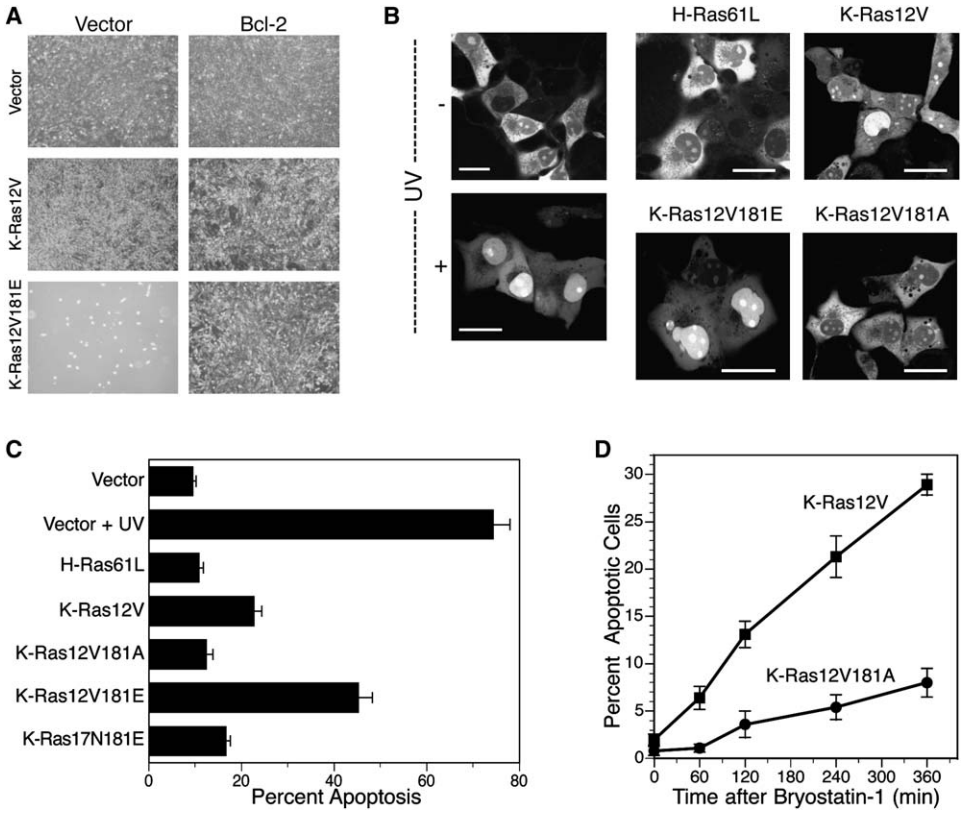

Figure 4. K-Ras with a Negative Charge at Position 181 Induces Apoptosis

(A) Expression of K-Ras12V181E in NIH3T3 cells induced cell death that was rescued by coexpression of Bcl-2.

(B and C) Apoptosis (measured as nuclear translocation of a caspase-3 biosensor) of COS-1 cells induced by UV irradiation or expression of the indicated Ras constructs (n = 4, $p < 0.0001$ K-Ras12v versus K-Ras12V181E).

(D) Bryostatin-1 stimulated apoptosis in NIH3T3 cells transformed with K-Ras12V but not K-Ras12V181A (n = 9, $p < 0.0001$ at each time).

overexpression of K-Ras12V resulted in a slightly elevated apoptotic index. Importantly, expression of K-Ras12V181E induced a high degree of apoptosis (Figures 4B and 4C). K-Ras12V181A that cannot be phosphorylated was less apoptotic than K-Ras12V, suggesting that the low-grade induction of apoptosis by oncogenic K-Ras in these cells is dependent on S181. K-Ras17N181E, predicted to be nucleotide free and therefore incapable of interacting with effectors, was inactive in the apoptosis assay, demonstrating a GTP dependence for the proapoptotic pathway (Figure 4C). Coexpression of the Raf-1 RBD with K-Ras12V181E inhibited apoptosis (data not shown), confirming that the effector binding domain of K-Ras12V181E is required to engage the proapoptotic pathway. K-Ras mutants in which the C-terminal polylysine sequence is changed to uncharged polyglutamine localize on the ER and Golgi but not mitochondria and do not affect cell viability (Choy et al., 1999; Hancock et al., 1990), suggesting that it is the mitochondrial localization of K-Ras phosphorylated on S181 that is required for apoptosis. The data suggest that relocalization of K-Ras from the PM to the mitochondria stimulates apoptosis via a GTP-dependent interaction on that organelle.

To confirm that K-Ras12V phosphorylated on S181, like phosphomimetic K-Ras12V181E, is proapoptotic, we examined the capacity of PKC agonists to induce apoptosis of K-Ras-transformed fibroblasts. Both bryostatin-1 (Figure 4D) and PMA plus ionomycin (data not shown) induced apoptosis to a much higher extent in cells transformed with K-Ras12V than those transformed with K-Ras12V181A. Thus, the sensitization to PKC-mediated apoptosis afforded by K-Ras transformation can be attributed to phosphorylation at S181.

K-Ras Interacts with Bcl-X_L on Mitochondria

Mounting evidence suggests that Ras can have proapoptotic effects in some cellular contexts (Cox and Der, 2003; Downward, 1998). The most compelling evidence has come from the characterization of a family of tumor suppressors that promote apoptosis and that have proven to be Ras effectors. The best characterized of these is Nore1 (Khokhlatchev et al., 2002). We found that a dominant-negative form of Nore1 (Khokhlatchev et al., 2002) had no effect on the ability of K-Ras12V181E to induce apoptosis, suggesting that phosphorylated K-Ras induces cell death via a Nore1-independent pathway.

Apoptosis can be mediated from intrinsic cellular pathways that originate from the ER and mitochondria (Breckenridge et al., 2003). Thus, the intracellular localizations of phosphorylated K-Ras include the cytoplasmic face of organelles intimately associated with apoptosis. The Bcl-2 family of proteins regulates apoptosis on these organelles. Apoptosis can be induced by augmenting the function of a proapoptotic Bcl-2

family member or by interfering with the function of an antiapoptotic member of the family. Ras has been reported to interact with Bcl-2 (Rebollo et al., 1999), suggesting that direct interaction with Bcl-2 or related proteins could mediate the proapoptotic affects of phosphorylated K-Ras. We examined by coimmunoprecipitation the capacity of K-Ras to associate with various Bcl-2 family proteins (Bcl-2, Bcl-X_L, Bak, Bax, and Bid). Although we confirmed association with Bcl-2, this interaction was insensitive to PKC agonists. In contrast, we observed that K-Ras associated with Bcl-X_L in a PKC-dependent fashion (Figures 5A and 5B). Moreover, K-Ras12V181E brought down 4.0- ± 0.8-fold ($n = 8$, $p < 0.005$) more Bcl-X_L than did K-Ras12V (Figures 5A and 5B). Nucleotide-free K-Ras17N181E was half as efficient as Ras12V181E in its ability to associate with Bcl-X_L, demonstrating that, in addition to the negative charge at position 181, the GTP binding state of K-Ras also contributes to the interaction. To confirm the interaction of K-Ras with endogenous Bcl-X_L, we used SW480 human colon cancer cells reported to express a relatively high level of Bcl-X_L (Krajewska et al., 1996) and found that endogenous Bcl-X_L interacted with K-Ras12V and that the interaction was enhanced by PKC agonists (Figure 5C).

To determine the compartment upon which K-Ras and Bcl-X_L interact, we examined cells expressing CFP-K-Ras12V and YFP-Bcl-X_L before and after stimulation with PKC agonists (Figures 5D and 5E). YFP-Bcl-X_L was observed constitutively on the outer mitochondrial membrane, and CFP-K-Ras12V colocalized with YFP-Bcl-X_L on that compartment following treatment with bryostatin-1 (Figure 5D) or PMA plus ionomycin (Figure 5E). To determine if this colocalization reflected an in vivo molecular interaction, we measured fluorescence resonance energy transfer (FRET) between the two fluorophors. By selectively photobleaching the acceptor (YFP-Bcl-X_L) on individual mitochondria and measuring a release of quenching of the donor (CFP-K-Ras), we detected FRET with an efficiency of 17% ± 8%, establishing a PKC-dependent molecular interaction between K-Ras and Bcl-X_L on the surface of mitochondria.

Apoptosis Stimulated by K-Ras12V181E Requires Bcl-X_L

To establish a functional interaction between proapoptotic K-Ras with a negative charge at position 181 and Bcl-X_L, we studied fibroblasts derived from embryos of mice null for Bcl-X_L or littermate controls. Staurosporine, etoposide, and calyculin A (data not shown) induced apoptosis to a similar degree in Bcl-$X_L^{+/+}$ and Bcl-$X_L^{-/-}$ cells, demonstrating that apoptotic pathways are intact in both cell types (data not shown). The fact that Bcl-X_L-deficient cells were not hypersensitive to proapoptotic drugs suggests that other antiapoptotic Bcl-2 family members compensate for the absence of Bcl-X_L. However, expression levels of Bcl-2 were similar in both cell types (see Figure S1 in the Supplemental Data available with this article online). In contrast to the proapoptotic drugs, K-Ras12V181E induced apoptosis in Bcl-$X_L^{+/+}$ but not Bcl-$X_L^{-/-}$ cells (Figure 6A). Strikingly, ectopic expression of Bcl-X_L (Figure 6B) restored the sensitivity of Bcl-$X_L^{-/-}$ cells to apoptosis induced by coexpressed K-Ras12V181E. Neither Bcl-2 nor Bcl-X_L lacking its C-terminal mitochondrial targeting sequence (Bcl-$X_L\Delta C$) could substitute for full-length Bcl-X_L in restoring sensitivity to K-Ras12V181E (Figure 6A). Expression of Bcl-$X_L\Delta C$ inhibited K-Ras12V181E-induced apoptosis in COS-1 cells (Figure 6C), confirming a role for Bcl-X_L in another cell type. To confirm that the results with phosphomimetic K-Ras reflected phosphorylation at position 181, we stably expressed K-Ras12V181S or K-Ras12V181A in Bcl-$X_L^{+/+}$ and Bcl-$X_L^{-/-}$ MEFs and studied the sensitivity of these cell lines to apoptosis induced by bryostatin-1. Bcl-$X_L^{+/+}$ cells expressing K-Ras12V181S but not K-Ras12V181A were sensitive. In contrast, Bcl-$X_L^{-/-}$ MEFs were resistant, regardless of which K-Ras allele was expressed (Figure 6D). Thus, Bcl-X_L is required for the induction of apoptosis by K-Ras phosphorylated at position 181.

K-Ras Is Required for Activation-Induced Cell Death of T Lymphocytes

Lymphocyte development and function require programmed cell death. Among the ways to induce apoptosis of T cells in vitro is to provide a strong stimulus through the TCR, a process known as activation-induced cell death (AICD). Because we observed that the same stimulus led to phosphorylation and internalization of K-Ras in T lymphocytes (Figures 2E and 2F), we asked if K-Ras was required for AICD. Jurkat T cells transfected with a pSUPER plasmid encoding an RNA hairpin efficient in silencing the *K-ras* gene (Figure S2) were protected from AICD, whereas the same cells transfected with a scrambled pSUPER were sensitive (Figure 6E). Because AICD is thought to be a surrogate for peripheral tolerance, these data suggest a role for K-Ras in this physiologically important form of apoptosis.

Bryostatin-1 Inhibits K-Ras-Driven Tumorigenesis in a S181-Dependent Manner

Our results suggest that, by promoting apoptosis, phosphorylation of oncogenic K-Ras on S181 might reverse cellular transformation and/or tumor progression. To test this idea, we studied the effect of bryostatin-1 on K-Ras-dependent transformation in vitro and in vivo. Bryostatin-1-inhibited K-Ras12V induced colony growth of fibroblasts in soft agar (Figure 7A). In contrast, soft agar growth induced by K-Ras12V181A was insensitive to bryostatin-1. Concordant with these in vitro results, tumors in nude mice established with fibroblasts transformed with K-Ras12V were sensitive to intraperitoneal administration of bryostatin-1, but tumors established with K-Ras12V181A-transformed fibroblasts were resistant (Figure 7B). TUNEL staining of the excised tumors revealed marked apoptosis of K-Ras12V-driven tumors treated with bryostatin-1, but tumors driven by K-Ras12V181A revealed little apoptosis (Figure 7C). Thus, the K-Ras farnesyl-electrostatic switch inhibits tumor growth in vivo by promoting programmed cell death.

Discussion

Peripheral membrane proteins have an advantage over transmembrane proteins in that their subcellular localization can be rapidly modulated. Many small GTPases take full advantage of this feature, moving on and off target membranes as part and parcel of their biological

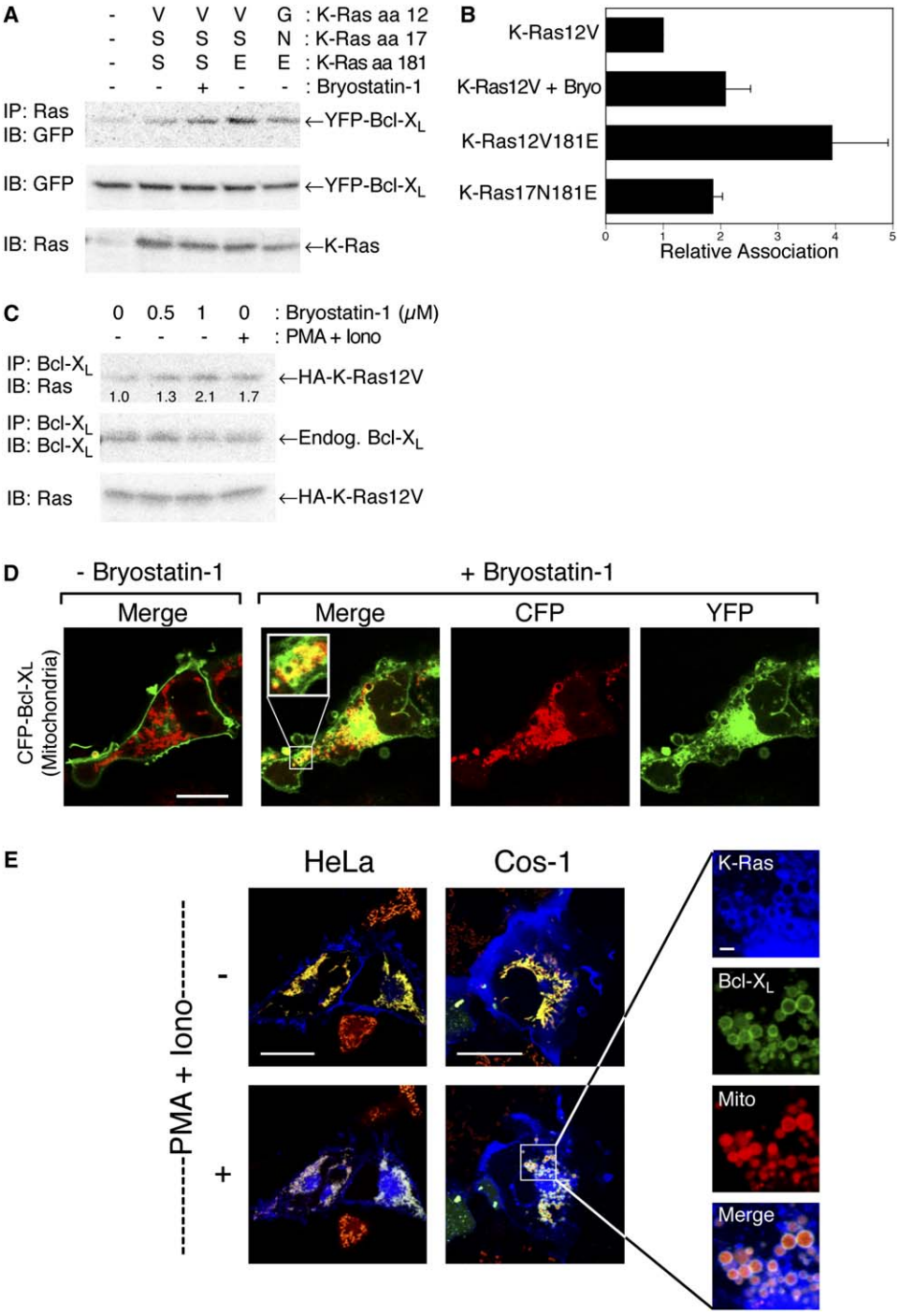

Figure 5. K-Ras Associates with Bcl-XL on Mitochondria

(A and B) Coimmunoprecipitation of YFP-Bcl-XL with indicated HA-K-Ras construct in COS-1 cells ± bryostatin-1 ($n = 8$, $p < 0.005$ for K-Ras12V versus K-Ras12V181E).

(C) Coimmunoprecipitation of K-Ras12V with endogenous Bcl-XL from SW480 human colon carcinoma cells.

(D) Colocalization of YFP-K-Ras12V (green) and CFP-Bcl-XL (red) on mitochondria of COS-1 cells treated with bryostatin-1 (5 min). The FRET efficiency between YFP-K-Ras12V and CFP-Bcl-XL on treated mitochondria (inset) was 17% ± 8%.

(E) Colocalization of YFP-K-Ras12V (blue) and CFP-Bcl-XL (green) on mitochondria (red) of HeLa and COS-1 cells treated with PMA plus ionomycin (5 min). Bars, 10 μm.

tasks. For example, many Rho and Rab family proteins cycle between membranes and their cytosolic chaperones as part of their activation process (Michaelson et al., 2001; Seabra and Wasmeier, 2004). In contrast, mature Ras proteins were thought until recently to associate irreversibly with the PM. This view is somewhat counterintuitive, since Ras proteins, unlike most Rho and Rab proteins, are modified with a single 15 carbon

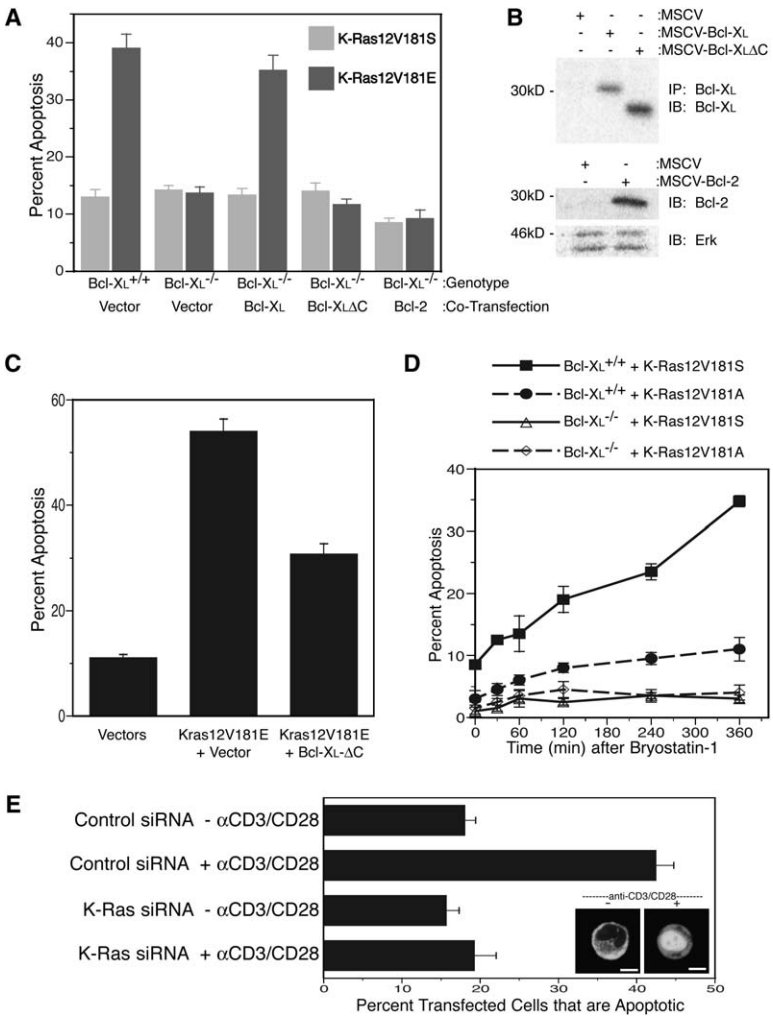

Figure 6. Apoptosis Induced by Phosphorylated K-Ras Is Dependent on Expression of Bcl-X_L, and AICD of T Cells Requires K-Ras

(A) Apoptosis measured by caspase-3 biosensor in Bcl-$X_L^{+/+}$ or Bcl-$X_L^{-/-}$ MEFs expressing the indicated K-Ras construct with or without coexpression of Bcl-X_L, Bcl-$X_L\Delta C$, or Bcl-2 ($n = 12$, $p < 0.0001$, Bcl-$X_L^{+/+}$ versus Bcl-$X_L^{-/-}$ expressing K-Ras12V181E).

(B) Equivalent expression of Bcl-X_L, Bcl-$X_L\Delta C$, and Bcl-2.

(C) Bcl-$X_L\Delta C$ inhibited K-Ras12V181E-induced apoptosis of COS-1 cells ($n = 4$, $p < 0.01$).

(D) Apoptosis following bryostatin-1 treatment of Bcl-$X_L^{+/+}$ or Bcl-$X_L^{-/-}$ MEFs expressing the indicated K-Ras construct ($n = 4$, $p < 0.001$, 360 min, K-Ras12V181E versus K-Ras12V181A in Bcl-$X_L^{+/+}$ and K-Ras12V181E in Bcl-$X_L^{+/+}$ versus Bcl-$X_L^{-/-}$).

(E) AICD (± anti-CD3/28) of Jurkat T cells measured by caspase-3 biosensor (inset) with or without silencing of K-Ras by siRNA ($n = 5$, $p < 0.001$).

farnesyl lipid rather than one or two 20 carbon geranylgeranyl lipids and thereby have less intrinsic affinity for membranes. Indeed, we have recently found that, whereas reversible carboxyl methylation of the C-terminal prenylcysteine that adds to its hydrophobicity is required for membrane association of Ras proteins, it is not required for Rho proteins (Michaelson et al., 2005), suggesting that the shorter prenyl modification evolved to afford relatively weak and reversible affinity for membranes.

It is now clear that the palmitoylated forms of Ras signal from endomembrane as well as the PM (Bivona et al., 2003; Chiu et al., 2002) and that a palmitoylation/depalmitoylation cycle (Magee et al., 1987) regulates bidirectional trafficking of these Ras isoforms between the Golgi and the PM (Goodwin et al., 2005; Rocks et al., 2005). Moreover, the retrograde trafficking from the PM to the Golgi of depalmitoylated Ras involves a cytosolic intermediate (Rocks et al., 2005), demonstrating conclusively that the farnesyl membrane anchor is relatively weak. Recently, K-Ras has been shown to translocate from the PM to the Golgi in hippocampal neurons stimulated with glutamate, and evidence was presented that the mechanism for K-Ras dissociation from the PM in this system was dependent on Ca^{2+}/calmodulin (Fivaz and Meyer, 2005). However, this mechanism is unlikely to account for the K-Ras translocation that we have observed. First of all, phosphorylation of even a single serine in the polybasic region MARCKS dramatically decreases Ca^{2+}/calmodulin binding by 200-fold (McIlroy et al., 1991), yet our data show conclusively that phosphorylation of S181 is required for translocation in response to PKC activation. Second, whereas PKC inhibitors blocked K-Ras translocation, Ca^{2+}/calmodulin inhibitors did not. We therefore favor a model that we have called the farnesyl-electrostatic switch, whereby the membrane affinity of K-Ras is modulated by phosphorylation within its polybasic region in a manner analogous to the myristoyl-electrostatic switch of the MARCKS protein. Phosphorylation at S181 acts to partially neutralize the charge and destabilize the electrostatic interaction with negatively charged phospholipid headgroups on the inner leaflet of the PM.

The sufficiency of a single phosphorylation event to trigger the K-Ras farnesyl-electrostatic switch suggests that the affinity of K-Ras for membranes is relatively weak, a conclusion supported by several in vitro observations. Seventy percent of GFP fused to a K-Ras tail could be extracted from cellular membranes with anionic phospholipid vesicles (Roy et al., 2000). Similarly, 70% of K-Ras was extracted from membrane vesicles with 0.25 M salt (Hancock et al., 1990). Substitution of

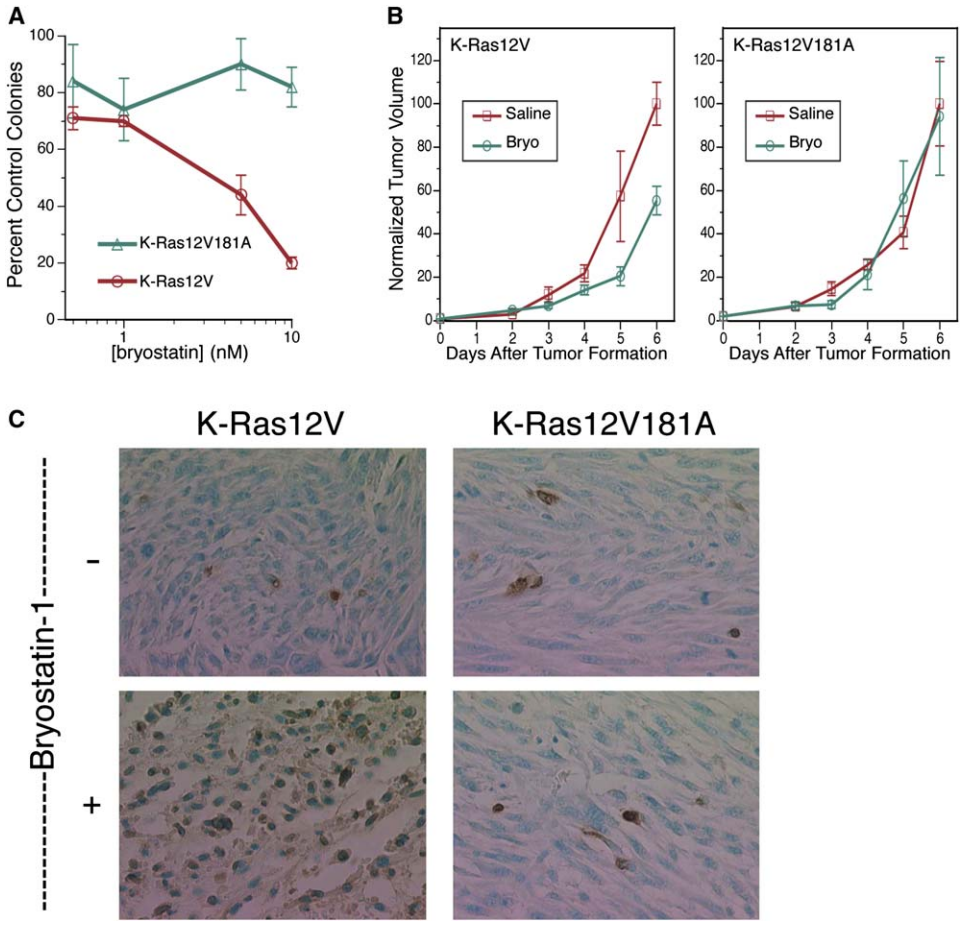

Figure 7. Phosphorylation Inhibits K-Ras12V-Mediated Transformation In Vitro and In Vivo

(A and B) S181 was required for inhibition by bryostatin-1 of (A) K-Ras12V-dependent growth in soft agar and (B) K-Ras12V-dependent tumor growth in nude mice. Only the curves representing K-Ras12V-dependent tumors ± bryostatin-1 were statistically different ($p < 0.05$, ANOVA). (C) TUNEL stain of tumors excised from animals treated as indicated with tumors driven by either K-Ras12V or K-Ras12V181A.

glutamine for two of the six contiguous lysines, the electrostatic equivalent of adding a phosphate group, resulted in recovery of 34% of K-Ras in the soluble fraction (Hancock et al., 1990). Our data reveal that 40% of total K-Ras can be extracted from total membrane fractions with isotonic cytosol. These data suggest that even a partial neutralization of the overall charge of the K-Ras polybasic region may be sufficient to significantly affect membrane affinity.

The Golgi and ER localization of phosphorylated K-Ras was not surprising, since K-Ras mutants with glutamines substituted for the lysines of the polybasic region were previously found on these compartments (Choy et al., 1999). Not so the mitochondrial localization that has not previously been observed in intact cells expressing GFP-tagged Ras proteins. The basis for the affinity of phosphorylated K-Ras for the outer mitochondrial membrane may reflect the phospholipid content of this compartment or the presence of a specific acceptor. Alternatively, or in addition, the interaction that we demonstrated between phospho-K-Ras and Bcl-X_L, a constitutive component of the outer mitochondrial membrane, may explain the affinity.

Although usually thought of as promoting cell growth and survival, the proapoptotic effects of Ras in some cellular contexts are well described (Cox and Der, 2003). Furthermore, isoform differences in the proapoptotic effects of Ras have been observed. For example, whereas K-Ras-transformed fibroblasts are sensitized to γ irradiation-induced apoptosis, H-Ras-transformed cells are protected (Choi et al., 2004). Our data demonstrate that activated K-Ras sensitizes cells to the proapoptotic effects of PKC agonists in an S181-dependent fashion. Combined with our demonstration that S181 is the principal PKC site on K-Ras, this offers compelling evidence for a proapoptotic function of K-Ras phosphorylated at S181. Our demonstration that activated K-Ras with a phosphomimetic substitution at position 181 potently induces apoptosis supports this conclusion. The finding that K-Ras phosphorylated on S181 is released from the PM and targets to the ER and mitochondria, organelles intimately involved in regulating apoptosis (Kuwana and Newmeyer, 2003; Scorrano et al., 2003), suggests a cell biological basis for the switch from a prosurvival to a proapoptotic molecule. Since K-Ras with a polyglutamine substitution for the polylysine sequence localizes to the ER but does not affect cell viability, we deduce that the mitochondrial-localized phospho-K-Ras is responsible for proapoptotic signaling.

K-Ras dissociated from the PM could trigger apoptosis, either by abruptly disengaging from prosurvival signaling down the PI3 kinase pathway or by engaging proapoptotic pathways (Cox and Der, 2003; Downward, 1998). The potent proapoptotic effect of K-Ras12V181E that we observed in cells with intact endogenous Ras signaling strongly suggests the latter. The best-studied proapoptotic Ras effectors are the RASSF family of tumor suppressors (Eckfeld et al., 2004). We found that a dominant-negative form of Nore1, the best-characterized member of this family (Khokhlatchev et al., 2002), was ineffective at blocking K-Ras12V181E-stimulated apoptosis. Because Ras proteins have been reported to interact with Bcl-2 family proteins (Rebollo et al., 1999), we explored the possibility that this type of interaction might mediate apoptosis and found that apoptosis induced by K-Ras phosphorylated at S181 requires Bcl-X_L.

Programmed cell death can be enhanced by positively regulating a proapoptotic Bcl-2 family (e.g., Bak, Bax, or Bid) member or inhibiting the action of an antiapoptotic family member (e.g., Bcl-2 and Bcl-X_L). Another intriguing possibility is the conversion of a generally antiapoptotic Bcl-2 family protein into a proapoptotic molecule. This has been shown to occur for Bcl-2 when it interacts with the nuclear orphan receptor Nur77/TR3 (Lin et al., 2004). In support of the potential for conversion of Bcl-2 is the observation that overexpression of this protein can stimulate programmed cell death (Uhlmann et al., 1998). Interestingly, whereas Bcl-2 targeted to the mitochondria can induce apoptosis, ER-targeted Bcl-2 cannot (Wang et al., 2001), establishing the mitochondria as the site of action of converted Bcl-2. The relatively weak interaction that we observed between phosphorylated K-Ras and Bcl-X_L makes less plausible a model in which phospho-K-Ras promotes apoptosis by stoichiometrically sequestering Bcl-X_L. On the other hand, a model in which phospho-K-Ras on the outer mitochondrial membrane converts Bcl-X_L to a proapoptotic protein is consistent with all of our data.

Removal of K-Ras from the PM may be a mechanism to acutely downregulate signaling for survival and growth. By promoting apoptosis, the K-Ras farnesyl-electrostatic switch can further act to limit the effects of K-Ras inappropriately activated by mutation or constitutive activation of upstream pathways. In support of this idea, we have found that a K-Ras allele devoid of phosphorylation sites in its C-terminal hypervariable region is hypertransforming (M.R.P. and A.D.C., unpublished data). Because all screening for *K-ras* mutations in human cancer has been limited to exons 1 and 2, it remains to be determined if codon 181 within exon 4B is a site for naturally occurring mutations in human cancer. In support of a physiologic role of K-Ras phosphorylation in promoting apoptosis, we have shown that AICD in T lymphocytes depends on K-Ras expression and that the conditions under which AICD is induced in these cells stimulate phosphorylation and translocation of endogenous Ras.

The proapoptotic pathway that we have characterized in this study is extremely significant, since it could be exploited to develop anticancer drugs that are specific for tumors driven by oncogenic K-Ras. We have tested this idea by assessing the anti-neoplastic effects of bryostatin-1, a PKC agonist already used in clinical trials (Kortmansky and Schwartz, 2003), in limiting the growth of K-Ras-dependent tumors. We found that, whereas bryostatin-1 was effective against tumors in nude mice derived from cells transformed with conventional oncogenic K-Ras12V, it lost its efficacy in tumors driven by K-Ras12V181A. This demonstrates that the antitumor action of bryostatin-1 was dependent on S181, the residue we found to be phosphorylated in response to the drug. This result suggests that agents that promote phosphorylation of K-Ras on S181 have the potential to be K-Ras-specific anticancer agents.

Experimental Procedures

Cell Culture, Transfection, and Metabolic Labeling

Cells were cultured and transfected (Bivona et al., 2003) and metabolically labeled with [^{32}P]orthophosphate (Ballester et al., 1987) as described. Details are also provided in Supplemental Data.

Cell Stimulation and Imaging

Cells were stimulated while under continuous observation by adding 100 nM bryostatin-1 (Biomol), 100 nM PMA with or without 500 ng/ml ionomycin, or 5 ng/ml anti-CD3 to 35 mm MatTek plates maintained at 37ºC using a PDMI-2 microincubator (Harvard Apparatus). Treatment of cells with 100 nM Ro 31-8220 (Biomol) or 15 μg/ml W-13 hydrochloride (EMD Biosciences) was initiated 10 min prior to stimulations. Where indicated, 25 pM MitoTracker Red CMXRos (Molecular Probes) was added 10 min prior to stimulation. Living cells were imaged with a Zeiss 510 inverted laser scanning confocal microscope. A minimum of five 0.45 μM Z slices were acquired for each cell at each time point, and representative images were chosen to display both PM and endomembranes. Unless otherwise stated, all images shown are representative of >90% of cells examined (10–100 cells examined per plate, $n \geq 6$). FRET on mitochondria between CFP-K-Ras and YFP-Bcl-X_L was detected by bleaching the acceptor (YFP-Bcl-X_L) on individual mitochondria and measuring the increase in CFP emission intensity as quenching was released. FRET efficiency was calculated as $[I_{CFP(postbleach)} - I_{CFP(prebleach)}]/I_{CFP(postbleach)}$. TIFF images were processed with Adobe Photoshop 7.0.

Immunogold Electron Microscopy

Jurkat cells (in suspension) were treated with 100 nM bryostatin-1 or vehicle (DMSO) for 30 min at 37ºC and then fixed with 2% formaldehyde and 0.2% glutaraldehyde in 0.1 M sodium phosphate buffer (pH 7.4). After washing in buffer, the cells were pelleted by centrifugation, embedded in 10% gelatin, cooled in ice, and cut into 1 mm^3 blocks. The blocks were infused with 2.3 M sucrose at 4ºC for at least 2 hr, frozen in liquid nitrogen, and stored until cryoultramicrotomy. Sections 100 nm thick were cut at −120ºC using an Ultracut T/FCS (Leica) equipped with an antistatic device (Diatome) and a diamond knife (Drukker). Ultrathin sections were picked up in a mix of 1.8% methylcellulose and 2.3 M sucrose (1:1) (Liou et al., 1996). Cryosections were collected on formvar-coated copper grids and incubated with Ras10 monoclonal antibody (Upstate) followed by rabbit anti-mouse antibodies and then protein A gold (Slot and Geuze, 1985). After labeling, the sections were treated with 1% glutaraldehyde, counterstained with uranyl acetate, and embedded in methyl cellulose-uranyl acetate (Slot et al., 1991). Images were acquired with a JEOL electron microscope JEM-1200 EX II at 80 kV.

Caspase-3 Activation

The assay was performed as described (Vos et al., 2003b).

Coimmunoprecipitation

COS-1 cells were cotransfected with GFP-tagged Bcl-2, Bcl-X_L, Bak, Bax, or Bid and either HA-tagged K-Ras12V, 12V181E, or 17N181E constructs. Twenty-four hours later, the cells were lysed and Ras was immunoprecipitated with Y13-259 rat monoclonal pan-Ras antibody. Immunoprecipitates were analyzed in duplicate by immunoblot with either Ras10 anti-Ras monoclonal antibody or anti-GFP polyclonal antiserum. To analyze endogenous Bcl-X_L,

SW480 cells were transfected with HA-tagged K-Ras12V and treated 24 hr later with vehicle, bryostatin-1, or PMA/ionomycin. The cells were then lysed in RIPA buffer containing protease inhibitors (Roche), microcystin, and NaF. Bcl-X_L was immunoprecipitated with anti-Bcl-X_L monoclonal antibody 7B2.5 and then collected on protein G beads. Immunoprecipitates were analyzed in duplicate by immunoblot with either anti-Bcl-X_L monoclonal antibody 13.6 or Ras10 anti-Ras monoclonal antibody. Immunoprecipitated proteins were detected by [^{125}I]protein A and quantified by PhosphorImager.

Activation-Induced Cell Death

Jurkat T cells (2×10^6) were transfected using DMRIE-C with 1.5 μg of YFP-caspase-3 sensor DNA and 5 μg of either pSuperRetro-Kras (K-Ras nt 25–43, 5′-GTTGGAGCTGGTGGCGTAG-3′) or pSuperRetro-Scrambled. Eighteen hours after transfection, the cells were stimulated with soluble anti-CD3 (1 μg/ml) and anti-CD28 (1 μg/ml) for an additional 54 hr. Transfected cells were imaged alive by epifluorescence microscopy on MatTek plates, and apoptosis was scored as nuclear fluorescence.

Soft Agar Assays

NIH 3T3 cells stably transfected with pCGN-hyg or the same vector encoding K-Ras12V or K-Ras12V181A were plated as single cell suspensions (2×10^4 cells per 35 mm well) in 0.4% agar over a bottom layer of 0.6% agar, both containing DMSO vehicle or various concentrations of bryostatin-1. After 2 weeks, the percentage of plated cells that formed colonies (>5 cell diameters across) was determined.

Tumor Growth Assays

NIH 3T3 cells stably transfected as per the soft agar assays were injected (5×10^5 cells) subcutaneously into the flanks of 4- to 6-week-old athymic nude BALB/c mice. After formation of palpable tumors, mice were treated daily for 3 days with intraperitoneal DMSO or bryostatin-1 (25 μg/kg). Tumor volume was measured daily, and differences in growth rates were evaluated for statistical significance by ANOVA.

Supplemental Data

Supplemental Data include Supplemental Experimental Procedures and two figures and can be found with this article online at http://www.molecule.org/cgi/content/full/21/4/481/DC1/.

Acknowledgments

We thank Angel Pellicer, Channing Der, and Richard Youle for thoughtful comments. We thank David Sabatini for assistance with immunogold EM. We thank Iwona Gumper for expert technical assistance. We thank Natalie Edmund for assistance with the tumorigenicity studies and Reggie Hill for TUNEL staining. This study was supported by grants from the National Institutes of Health (to M.R.P. and A.D.C.), the New York State Breast Cancer Research Program, the Burroughs Wellcome Fund (to M.R.P.), and the Lustgarten Foundation for Pancreatic Cancer Research (to A.D.C.).

Received: May 15, 2005
Revised: December 12, 2005
Accepted: January 5, 2006
Published: February 16, 2006

References

Ballester, R., Furth, M.E., and Rosen, O.M. (1987). Phorbol ester- and protein kinase C-mediated phosphorylation of the cellular Kirsten ras gene product. J. Biol. Chem. *262*, 2688–2695.

Bivona, T.G., Perez De Castro, I., Ahearn, I.M., Grana, T.M., Chiu, V.K., Lockyer, P.J., Cullen, P.J., Pellicer, A., Cox, A.D., and Philips, M.R. (2003). Phospholipase Cγ activates Ras on the Golgi apparatus by means of RasGRP1. Nature *424*, 694–698.

Bos, J.L. (1989). ras oncogenes in human cancer: a review. Cancer Res. *49*, 4682–4689.

Breckenridge, D.G., Germain, M., Mathai, J.P., Nguyen, M., and Shore, G.C. (2003). Regulation of apoptosis by endoplasmic reticulum pathways. Oncogene *22*, 8608–8618.

Chiu, V.K., Bivona, T., Hach, A., Sajous, J.B., Silletti, J., Wiener, H., Johnson, R.L., Cox, A.D., and Philips, M.R. (2002). Ras signalling on the endoplasmic reticulum and the Golgi. Nat. Cell Biol. *4*, 343–350.

Choi, J.A., Park, M.T., Kang, C.M., Um, H.D., Bae, S., Lee, K.H., Kim, T.H., Kim, J.H., Cho, C.K., Lee, Y.S., et al. (2004). Opposite effects of Ha-Ras and Ki-Ras on radiation-induced apoptosis via differential activation of PI3K/Akt and Rac/p38 mitogen-activated protein kinase signaling pathways. Oncogene *23*, 9–20.

Choy, E., Chiu, V.K., Silletti, J., Feoktistov, M., Morimoto, T., Michaelson, D., Ivanov, I.E., and Philips, M.R. (1999). Endomembrane trafficking of ras: the CAAX motif targets proteins to the ER and Golgi. Cell *98*, 69–80.

Cox, A.D., and Der, C.J. (2003). The dark side of Ras: regulation of apoptosis. Oncogene *22*, 8999–9006.

Downward, J. (1998). Ras signalling and apoptosis. Curr. Opin. Genet. Dev. *8*, 49–54.

Downward, J., Graves, J.D., Warne, P.H., Rayter, S., and Cantrell, D.A. (1990). Stimulation of p21ras upon T-cell activation. Nature *346*, 719–723.

Eckfeld, K., Hesson, L., Vos, M.D., Bieche, I., Latif, F., and Clark, G.J. (2004). RASSF4/AD037 is a potential ras effector/tumor suppressor of the RASSF family. Cancer Res. *64*, 8688–8693.

Fivaz, M., and Meyer, T. (2005). Reversible intracellular translocation of KRas but not HRas in hippocampal neurons regulated by Ca2+/calmodulin. J. Cell Biol. *170*, 429–441.

Goodwin, J.S., Drake, K.R., Rogers, C., Wright, L., Lippincott-Schwartz, J., Philips, M.R., and Kenworthy, A.K. (2005). Depalmitoylated Ras traffics to and from the Golgi complex via a nonvesicular pathway. J. Cell Biol. *170*, 261–272.

Hancock, J.F., Paterson, H., and Marshall, C.J. (1990). A polybasic domain or palmitoylation is required in addition to the CAAX motif to loacalize $p21^{ras}$ to the plasma membrane. Cell *63*, 133–139.

Jackson, J.H., Li, J.W., Buss, J.E., Der, C.J., and Cochrane, C.G. (1994). Polylysine domain of K-ras 4B protein is crucial for malignant transformation. Proc. Natl. Acad. Sci. USA *91*, 12730–12734.

Khokhlatchev, A., Rabizadeh, S., Xavier, R., Nedwidek, M., Chen, T., Zhang, X.F., Seed, B., and Avruch, J. (2002). Identification of a novel Ras-regulated proapoptotic pathway. Curr. Biol. *12*, 253–265.

Kortmansky, J., and Schwartz, G.K. (2003). Bryostatin-1: a novel PKC inhibitor in clinical development. Cancer Invest. *21*, 924–936.

Krajewska, M., Moss, S.F., Krajewski, S., Song, K., Holt, P.R., and Reed, J.C. (1996). Elevated expression of Bcl-X and reduced Bak in primary colorectal adenocarcinomas. Cancer Res. *56*, 2422–2427.

Kuwana, T., and Newmeyer, D.D. (2003). Bcl-2-family proteins and the role of mitochondria in apoptosis. Curr. Opin. Cell Biol. *15*, 691–699.

Lang, P., Gesbert, F., Delespine-Carmagnat, M., Stancou, R., Pouchelet, M., and Bertoglio, J. (1996). Protein kinase A phosphorylation of RhoA mediates the morphological and functional effects of cyclic AMP in cytotoxic lymphocytes. EMBO J. *15*, 510–519.

Lerosey, I., Pizon, V., Tavitian, A., and de Gunzburg, J. (1991). The cAMP-dependent protein kinase phosphorylates the rap1 protein in vitro as well as in intact fibroblasts, but not the closely related rap2 protein. Biochem. Biophys. Res. Commun. *175*, 430–436.

Leventis, R., and Silvius, J.R. (1998). Lipid-binding characteristics of the polybasic carboxy-terminal sequence of K-ras4B. Biochemistry *37*, 7640–7648.

Lin, B., Kolluri, S.K., Lin, F., Liu, W., Han, Y.H., Cao, X., Dawson, M.I., Reed, J.C., and Zhang, X.K. (2004). Conversion of Bcl-2 from protector to killer by interaction with nuclear orphan receptor Nur77/TR3. Cell *116*, 527–540.

Liou, W., Geuze, H.J., and Slot, J.W. (1996). Improving structural integrity of cryosections for immunogold labeling. Histochem. Cell Biol. *106*, 41–58.

Magee, A.I., Gutierrez, L., McKay, I.A., Marshall, C.J., and Hall, A. (1987). Dynamic fatty acylation of p21N-ras. EMBO J. *6*, 3353–3357.

McIlroy, B.K., Walters, J.D., Blackshear, P.J., and Johnson, J.D. (1991). Phosphorylation-dependent binding of a synthetic MARCKS peptide to calmodulin. J. Biol. Chem. *266*, 4959–4964.

McLaughlin, S., and Aderem, A. (1995). The myristoyl-electrostatic switch: a modulator of reversible protein-membrane interactions. Trends Biochem. Sci. *20*, 272–276.

Michaelson, D., Silletti, J., Murphy, G., D'Eustachio, P., Rush, M., and Philips, M.R. (2001). Differential localization of Rho GTPases in live cells. Regulation by hypervariable regions and RhoGDI binding. J. Cell Biol. *152*, 111–126.

Michaelson, D., Ali, W., Chiu, V.K., Bergo, M., Silletti, J., Wright, L., Young, S.G., and Philips, M. (2005). Postprenylation CAAX processing is required for proper localization of Ras but not Rho GTPases. Mol. Biol. Cell *16*, 1606–1616.

Quilliam, L.A., Mueller, H., Bohl, B.P., Prossnitz, V., Sklar, L.A., Der, C.J., and Bokoch, G.M. (1991). Rap1A is a substrate for cyclic AMP-dependent protein kinase in human neutrophils. J. Immunol. *147*, 1628–1635.

Rebollo, A., Perez-Sala, D., and Martinez, A.C. (1999). Bcl-2 differentially targets K-, N-, and H-Ras to mitochondria in IL-2 supplemented or deprived cells: implications in prevention of apoptosis. Oncogene *18*, 4930–4939.

Rocks, O., Peyker, A., Kahms, M., Verveer, P.J., Koerner, C., Lumbierres, M., Kuhlmann, J., Waldmann, H., Wittinghofer, A., and Bastiaens, P.I. (2005). An acylation cycle regulates localization and activity of palmitoylated Ras isoforms. Science *307*, 1746–1752.

Roy, M.O., Leventis, R., and Silvius, J.R. (2000). Mutational and biochemical analysis of plasma membrane targeting mediated by the farnesylated, polybasic carboxy terminus of K-ras4B. Biochemistry *39*, 8298–8307.

Scorrano, L., Oakes, S.A., Opferman, J.T., Cheng, E.H., Sorcinelli, M.D., Pozzan, T., and Korsmeyer, S.J. (2003). BAX and BAK regulation of endoplasmic reticulum Ca2+: a control point for apoptosis. Science *300*, 135–139.

Seabra, M.C., and Wasmeier, C. (2004). Controlling the location and activation of Rab GTPases. Curr. Opin. Cell Biol. *16*, 451–457.

Sidhu, R.S., Clough, R.R., and Bhullar, R.P. (2003). Ca2+/calmodulin binds and dissociates K-RasB from membrane. Biochem. Biophys. Res. Commun. *304*, 655–660.

Slot, J.W., and Geuze, H.J. (1985). A new method of preparing gold probes for multiple-labeling cytochemistry. Eur. J. Cell Biol. *38*, 87–93.

Slot, J.W., Geuze, H.J., Gigengack, S., Lienhard, G.E., and James, D.E. (1991). Immuno-localization of the insulin regulatable glucose transporter in brown adipose tissue of the rat. J. Cell Biol. *113*, 123–135.

Szallasi, Z., Smith, C.B., Pettit, G.R., and Blumberg, P.M. (1994). Differential regulation of protein kinase C isozymes by bryostatin 1 and phorbol 12-myristate 13-acetate in NIH 3T3 fibroblasts. J. Biol. Chem. *269*, 2118–2124.

Uhlmann, E.J., Subramanian, T., Vater, C.A., Lutz, R., and Chinnadurai, G. (1998). A potent cell death activity associated with transient high level expression of BCL-2. J. Biol. Chem. *273*, 17926–17932.

Valge, V.E., Wong, J.G., Datlof, B.M., Sinskey, A.J., and Rao, A. (1988). Protein kinase C is required for responses to T cell receptor ligands but not to interleukin-2 in T cells. Cell *55*, 101–112.

Villalonga, P., Lopez-Alcala, C., Bosch, M., Chiloeches, A., Rocamora, N., Gil, J., Marais, R., Marshall, C.J., Bachs, O., and Agell, N. (2001). Calmodulin binds to K-Ras, but not to H- or N-Ras, and modulates its downstream signaling. Mol. Cell. Biol. *21*, 7345–7354.

Vos, M.D., Ellis, C.A., Elam, C., Ulku, A.S., Taylor, B.J., and Clark, G.J. (2003a). RASSF2 is a novel K-Ras specific effector and potential tumor suppressor. J. Biol. Chem. *278*, 28045–28051.

Vos, M.D., Martinez, A., Ellis, C.A., Vallecorsa, T., and Clark, G.J. (2003b). The Pro-apoptotic Ras effector Nore1 may serve as a Ras-regulated tumor suppressor in the lung. J. Biol. Chem. *278*, 21938–21943.

Wang, N.S., Unkila, M.T., Reineks, E.Z., and Distelhorst, C.W. (2001). Transient expression of wild-type or mitochondrially targeted Bcl-2 induces apoptosis, whereas transient expression of endoplasmic reticulum-targeted Bcl-2 is protective against Bax-induced cell death. J. Biol. Chem. *276*, 44117–44128.